Macromolecular Research, Vol. 17, No. 3, pp 181-186 (2009)

Ordered Micropatterns by Confined Dewetting of an Imprinted Polymer Thin Film and Their Microlens Application

Geuntak Lee, Bokyung Yoon, Himadri Acharya, and Cheolmin Park*

Department of Materials Science and Engineering, Yonsei University, Seoul 120-749, Korea

June Huh

Department of Materials Science and Engineering, Seoul National University, Seoul 151-742, Korea

Received July 23, 2008; Revised September 5, 2008; Accepted September 5, 2008

Abstract: We fabricated ordered micro/nano patterns induced by controlled dewetting on the topographically patterned PS/P4VP bilayer thin film. The method is based on utilizing microimprinting lithography to induce a topographically heterogeneous bilayer film that allows the controlled dewetting upon subsequent thermal annealing. The dewetting that was initiated strictly at the boundary of the thicker and thinner regions was guided by the presence of the topographic structure. The dewetting front velocity of the microdomains in the confined regions was linearly proportional to the measurement time, which enabled us to control the size of the dewet domain with annealing time. In particular, the submicron sized dot arrays between lines were generated with ease when the dewetting was confined into geometry with a few microns in size. The kinetically driven, non-lithographical pattern structures accompanied the pattern reduction to 400%. The pattern arrays on a transparent glass substrate were especially useful for non-circular microlens arrays where the focal length of the lens was easily tunable by controlling the thermal annealing.

Keywords: dewetting, microimprinting, bilayer, self-assembly, microlens, micropattern.

Introduction

Generation of the controlled micro/nano patterns on a substrate is of the enormous importance of both fundamental research and practical objects such as electronic chip production, microfluidics, and bio-sensor.[1-3] The problems including high cost and time consuming confronted by the conventional lithography for manufacturing nanostructure may be resolved by using soft lithographic techniques in particular combined with various self organization driving forces of polymers including macro-phase separation in blends, micro-phase separation in block copolymers and dewetting.[4-7]

The morphology of a thin polymer film on either solid or liquid can be evolved by the instability into the film resulting from its interaction with the substrate of long range force of van der Waals, short range polar and molecular force. This usual method for morphology evolution on a flat surface is the dewetting in which an initially uniform film on a non-wetting substrate ruptures into droplets. Meanwhile, the mechanism for the rupture of thin polymer film is elucidated by e.g., spinodal dewetting, nucleation and growth dewetting.[8] In spinodal dewetting, the unstable growth of capillary waves induces spontaneous rupture of the film with the long range molecular forces. Nucleation and growth in contrast involves the nucleation of holes on the defect sites of the film and subsequent growth of the holes with the consequent formation of rims, polygons and droplets.

The pursuit of dewetting may also provide novel method as a means of generating ordered micropatterned morphology, although it is in general considered problematic in many applications.[9,10] A number of publications have demonstrated the potentials of controlling dewetting for ordered micron pattern fabrication in polymer, metal thin film and nanoparticle solution.[4-6,11,12] In our previous work, we have demonstrated a kinetically driven and non-lithogrpahic method for fabricating ordered microstructures of polymers by combining dewetting with microimprinting lithography. The proper thermal treatment of a microimprinted poly4vinylpyridine (P4VP)/polystyrene (PS) bilayer on a Si substrate allowed the confined dewetting selectively in the pressed thinner regions. The subsequent prolong annealing additionally enabled us to induce the layer inversion between PS and P4VP layer, giving rise to an ordered dewet structure with both chemical and topological heterogenity in large area.[7]

In this contribution, we present the details of the formation of the ordered dewet structures upon heat treatment with *in-situ* optical microscope. The kinetics of the confined dewetting

*Corresponding Author. E-mail: cmpark@yonsei.ac.kr

of P4VP layer on PS surface is investigated in the imprinted bilayer with various pattern symmetries as a function of film thickness and annealing temperature. For a potential application of the ordered dewet patterns, we also demonstrate optical microlens arrays fabricated from our unconventional lithographic technique whose focal length is beneficially tunable by controlling the thermal annealing with ease.

Experimental

Materials and Bilayer Preparation. We employed a polystyrene (PS) and a poly(4vinyl pyridine) (P4VP) purchased from Polymer Source Inc., Doval, Canada. The molecular weights of PS and P4VP are 45,800 g/mol and 48,000 g/mol, respectively and the polydispersity of both polymers is about 1.05. To prepare a bilayer thin film, a 2 wt% PS solution in toluene was first spin coated onto a silicon substrate and a 2 wt% P4VP solution in ethyl alcohol was spin coated on the PS film. The silicon wafers (100) were rinsed with acetone, methanol, and deionized water in order, then dried with N_2 for cleaning. The spin coating (Spin coater: SPIN 1200 Midas-system, Korea) was carried out at the 2,000 rpm for 1 min at room temperature for each polymer. The thicknesses of PS and P4VP film prepared were approximately 80 and 100 nm, respectively.

Micro-Imprinting Lithography. The spin coated P4VP/PS bilayer was topographically patterned with the micro-imprinting apparatus developed in our laboratory. The heater is located beneath a metallic sample stage with the temperature range from room temperature to 300 °C. The bilayer on a substrate fixed on the sample holder moves upward by the moving stage connected to a micro-motor. When the conformal contact is formed with a poly(dimethylsiloxane) (PDMS) master pattern, the temperature is raised above the glass transition temperatures of both polymers (150 °C). The load cell (maximum load: 2 kg) located above the master pattern holder controls the pressure applied during micro-imprinting. The pressure applied depends on both the load and the contact area of the micropattern on the bilayer. The pressure used is approximately 156,800 Pa. The micro-imprinting under the pressure at 150 °C was performed for 15 min, resulting in the micropatterns with topographic thickness variation in large areas (1×1 cm^2). The elastomeric PDMS mold was fabricated by curing a PDMS precursor (Sylgard 184, Dow Corning Corp) on a prepatterned silicon master. Two kinds of PDMS molds were used. One is 1 dimensional periodic line with the width and periodicity of 2 and 4 μm, respectively. The other is a 2 dimensional PDMS mold that has hexagonal holes with 15 μm in size arrayed into a hexagonal structure. The center-to-center distance between two holes is 25 μm.

Confined Dewetting and Characterization. Topographically micropatterned bilayer by micro imprinting was annealed at 200 and 230 °C for dewetting the top P4VP layer in the selective areas. After annealing for less than 5 min the dewetting of the P4VP layer occurred only in the thinner regions and unique micropatterns were observed. The procedure of our patterning method is schematically depicted in Figure 1. The temperature of the dewetting was controlled by a thermal stage from Linkem (THMSE 600). The dynamics of the dewetting was monitored by optical microscope (Olympus BX 51M) in reflection mode with CCD camera (PL-A662 provided by Pixelink). The surface structure of the micropatterns was characterized with SEM (Hitachi: S-2700) operated at 10 kV. AFM (Nanoscope III from Digital Instrument) was used in tapping mode to obtain the information of the pattern surface and film thickness.

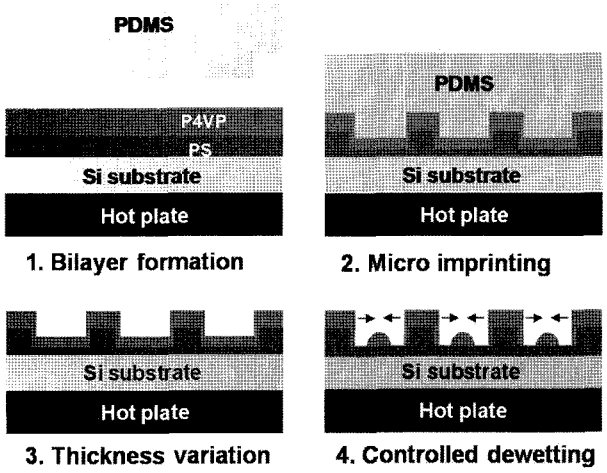

Figure 1. Procedure of the controlled dewetting. Micro-imprinting on a P4VP/PS bilayer induces thickness variation. The subsequent temperature annealing confines the dewetting of the P4VP layer only in the thinner regions.

Results and Discussion

We have applied the PDMS mold where hexagonal holes are arrayed with 6 mm hexagonal symmetry. The imprinting on a P4VP/PS bilayer with the PDMS mold produced well defined hexagonal posts with 6 mm symmetry shown in Figure 2(a). A SEM micrograph in inset of Figure 2(a) exhibits that the top surface of each hexagonal post is concave due to the insufficient material filling.[13] Punched bilayer film was examined by AFM in height contrast. Height difference between the elevated regions and the punched ones is approximately 250 nm and the surface of the punched regions looks flat. When P4VP layer was selectively removed by ethanol the punched regions clearly exhibit the parabolic surface profile where punched pattern boundary is thinner than center. It confirms the local capillary flow at the vicinity of pattern boundary during micro-imprinting.[13]

The dewetting dynamics was monitored by consecutive optical microscope images obtained with time t. The representative images captured during the dewetting are shown

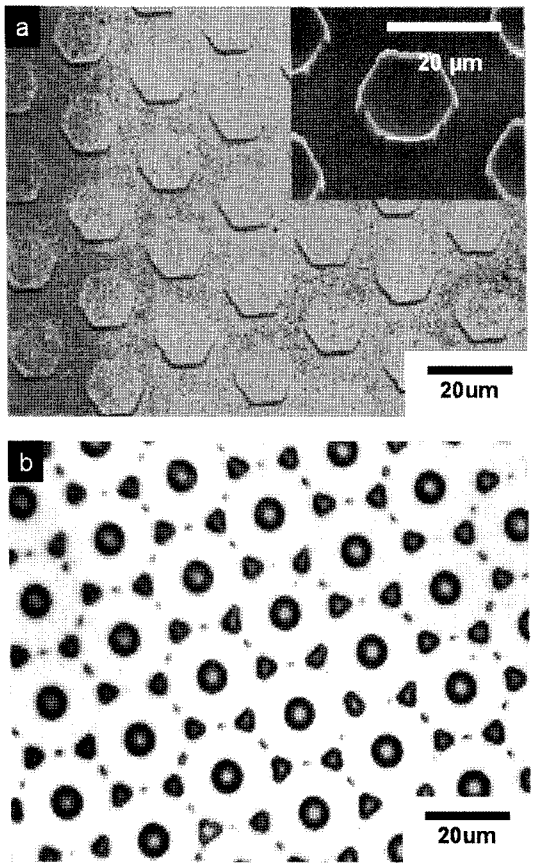

Figure 2. The controlled dewetting of a micro-imprinted P4VP/PS bilayer film on a Si substrate with a PDMS mold that has hexagonal holes with 6 mm hexagonal symmetry. OM (a) and SEM (inset of (a)) images of the imprinted P4VP/PS bilayer pattern. (b) OM image of the imprinted P4VP/PS bilayer after controlled dewetting. The dewetting in the thinner inside and outside regions produced a new micropattern with hemi-spherical and triangular features.

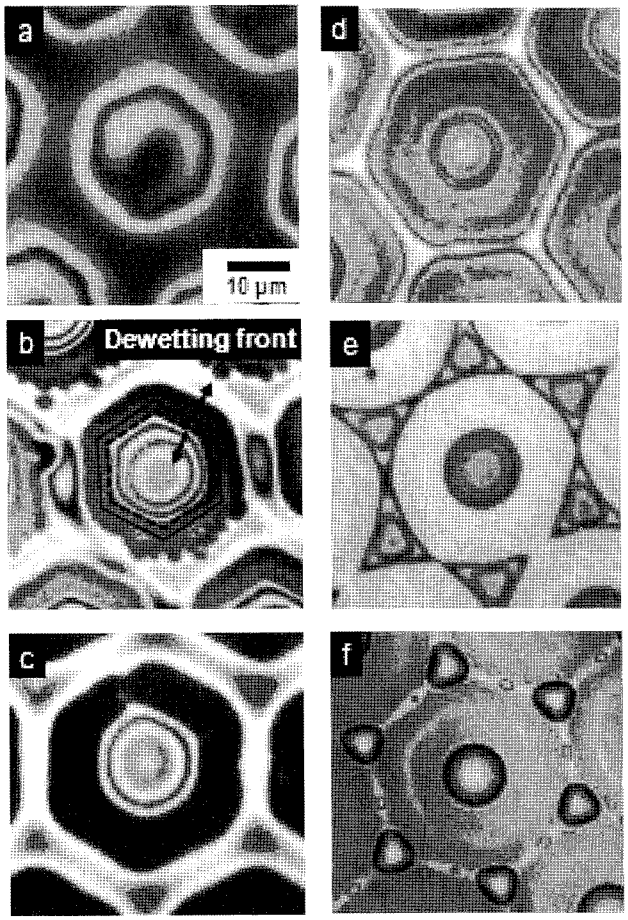

Figure 3. OM images representing morphological evolution with time in the micro-imprinted 15 μm hexagonal patterns of the P4VP/PS bilayer shown as at 200 °C (a) Imprinted pattern before annealing. (b) Initiation of dewetting. Dotted and solid lines display the dewetting initiation boundary following arrows. (c), (d) Hexagonal type polygon formation. (e) Triangular shape structure formation around the hemi-spherical feature. (f) The final morphology after annealing. The scale bar is 10 μm.

in Figure 3. The film thickness of the center regions of the hexagonal posts was found almost the same as one of outer parts as confirmed by a height mode AFM image analysis (~ 80 nm). Therefore, the subsequent dewetting of the P4VP layer occurred simultaneously in both inside and outside of the posts. In the inside of the posts, the dewetting began at the boundary as depicted with dotted line in Figure 3(b) and propagated toward the center, resulting in hemi-spherical dots. In outer regions the dewetting initiated at the boundary of the posts, as illustrated by a solid line in Figure 3(b), was guided by the presence of the arrays of the hexagonal posts. We obtained a honeycomb shape polygon structure of the dewetting P4VP layer as shown in Figures 3(c) and (d), contrary to a randomized polygon one typically observed in dewetting of polymer thin films.[8,14] Further heat treatment broke the polygon scaffold into ellipsoids and triangular droplets with 6 mm symmetry (Figures 3(e) and (f)). The arrays of the P4VP microdomains are shown after the controlled dewetting in Figure 2(b).

We found that the velocity of dewetting front described as dL/dt was constant at the annealing temperature of 200 and 230 °C as shown in Figure 4, where L is the length from the center of a hexagonal pattern to the outer point of a propagating hole. Our observation is consistent with others where the hole radius increased with time linearly. The dewetting front velocity of P4VP layer becomes much faster at 230 °C, which implies that the hole growth rate is a function of temperature as addressed in the dewetting of homogeneous thin films.[15,16] The velocity of dewetting estimated with the slope of each linear fitting (dL/dt) is approximately 3.3 and 0.55 μm/sec at 230 and 200 °C, respectively. It should be noted that the facile control of the size and shape of the dewetting domains with both time and temperature is beneficial for fabricating sphere cap and triangular shaped

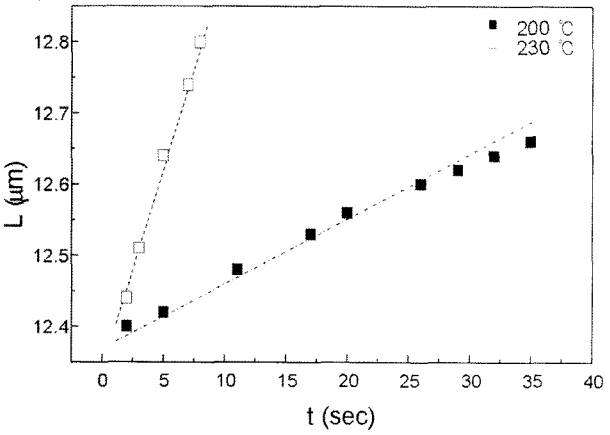

Figure 4. Plot of the center to dewet front distance as a function of time at the different annealing temperature. The velocity of dewetting described as *dL/dt* is obtained by the slope of linear fitting.

microlens arrays with different focal length as shown later.

Figure 5(a) shows the OM image of P4VP/PS bilayers micro-imprinted by PDMS molds with periodic lines. The micro-imprinting again induced thickness variation of a bilayer. The maximum height of the elevated region is approximately 250 nm, and that of punched, thinner region is approximately 80 nm; each layer has approximately 40 nm in thickness measured by AFM. The selective dewetting produced an interesting sub-micron pattern selectively in the thinner regions where a broken line pattern was observed with approximately 500 nm in width as shown in Figures 5(b) and 5(c). Approximtely 400% pattern reduction arising from the controlled dewetting renders our method very effective to fabricate sub-micro polymer patterns with ease.

It should be noted that the pattern structure we obtained is thermodynamically unstable, but kinetically driven. According to Brochard-Wyart *et al.*,[14] a critical thickness (e_c), below which an upper layer (A-layer) is unstable against dewetting on a liquid substrate (B-layer) is given as $e_c = 2[\gamma/(\rho g)]^{1/2} \sin(\theta_E/2)$ where g is the gravitational constant, θ_E is the angle of a liquid wedge, and the effective parameters for surface tension γ and density ρ are given by $\gamma^{-1} = \gamma_A^{-1} + \gamma_{AB}^{-1}$ and $\rho = \rho_A \rho_B^{-1}(\rho_B - \rho_A)$. A rough estimation based on the parameters reported previously for PS/P4VP system gives e_c as an order of 100 nm.[7] Nevertheless, for the experimental conditions in this study, the dewetting did not occur at the elevated (thicker) region and the structure became stable when it was vitrified below the glass transition temperatures of both polymers. Hence, it is certain that the elevated areas with approximately 250 nm in thickness shown in Figure 5(a) will be eventually broken up at certain time and temperature scale.

We also performed the dewetting on the pre-patterned P4VP/PS bilayer prepared on a glass substrate. As shown in Figure 6(a), the controlled micropattern successfully obtained on the glass substrate is useful for unconventional micro-

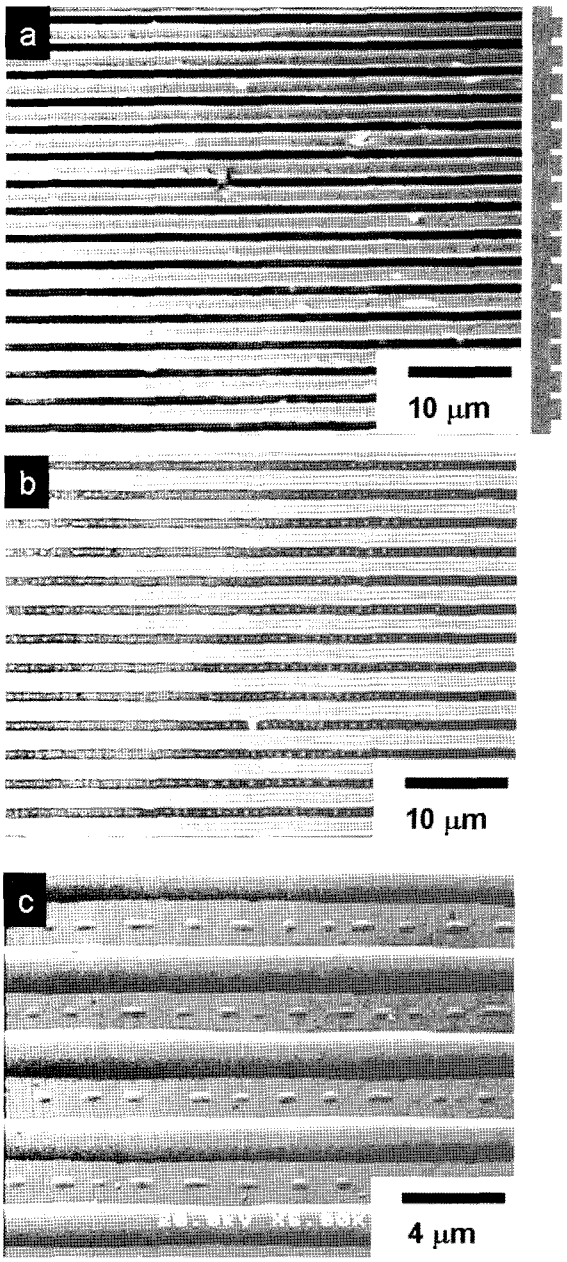

Figure 5. The controlled dewetting of a micro-imprinted P4VP/PS bilayer film on a Si substrate with a PDMS mold having 2 and 4 μm in width and periodicity, respectively. (a) OM image of the imprinted P4VP/PS bilayer pattern. OM (b) and SEM (c) images of the P4VP/PS bilayer pattern after the thermal annealing. The dewetting occurred only in thinner regions in between the elevated line patterns.

lenses. We used an optical microscope to characterize the lensing of the microlenses under white-light illumination. The optical system for characterizing the microlensing is illustrated in Figure 6(b). Figures 6(c) and (d) show the focused images by the microlenses produced by the micropattern corresponding to Figure 6(a). Since the height and profile of the spherical shape microlenses is different from that of the

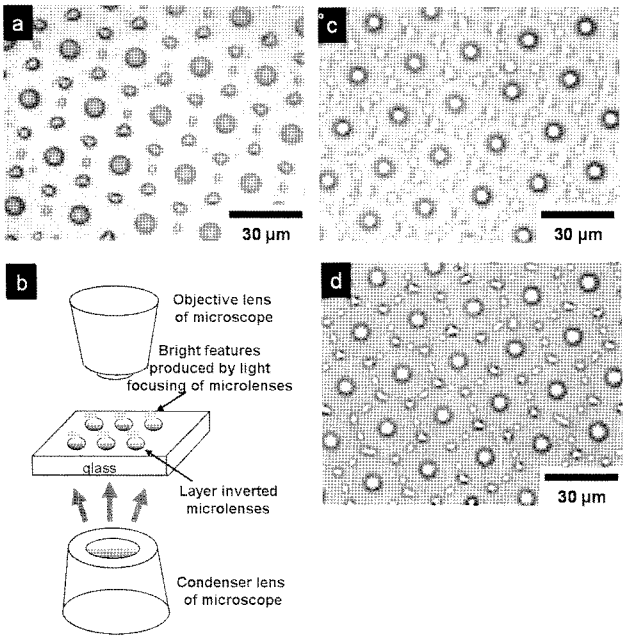

Figure 6. The controlled dewetting of a micro-imprinted P4VP/PS bilayer film on a glass substrate with the PDMS mold used in Figure 2(a) OM image of the P4VP/PS bilayer pattern after thermal annealing. (b) Schematic of micro-lensing of the microlenses obtained by the controlled dewetting under white-light illumination. Focused OM images produced by the spherical (c) and the triangular (d) microlenses, respectively.

ellipsoids and the triangular ones, the location of the focal planes is varied along the direction perpendicular to the micropattern array surface. The focused images with the focal planes of spherical and triangular lenses are shown in Figures 6(c) and (d), respectively.[17]

The focal length of the circular microlens shown for example in Figure 6(a) can be in particular easily tuned by controlling thermal annealing time. For an interface with surface tension γ, the Young–Laplace equation shows the pressure difference maintained by the surface: $\Delta p = 2\gamma_{LG}/R$, where Δp is the pressure difference between internal and external spherical surface, γ_{LG} and R are the surface tension

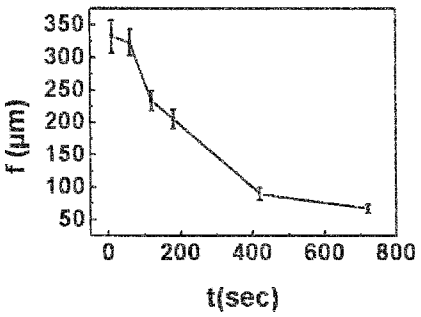

Figure 7. The calculated focal length of a microlens produced by the controlled dewetting of a PS/P4VP bilayer with annealing time at 200 °C.

of the liquid and the radius of curvature of sphere, respectively. Focal length, f of lens as function of pressure is given by $f = (2\gamma_{LG})/(\Delta n \Delta p)$ where Δn is the difference of refractive indices between liquid and air. Combining the focal length equation with the previous relation of Δp, a simple formula about focal length related to radius of curvature can be written as $f = R/\Delta n$.[18] After all, the focal length is controllable by the radius of curvature. Figure 7 shows the modulation of the focal length of the circular microlenses by controlling the dewetting time of a PS/P4VP bilayer at 200 °C. In our system, the focal length of a P4VP microlens is varied from 332 to 67 μm with n_{P4VP} of 1.6[19] by the simple controlled dewetting within 720 sec.

Conclusions

We demonstrated a new method to fabricating the ordered patterns of micro-imprinted P4VP/PS bilayer using the confined dewetting. The microimprinting produced a topographic pattern with the thickness variation which guided the subsequent dewetting of P4VP layer of the P4VP and PS bilayer on a Si substrate. The initiation of the dewetting occurred strictly at the boundary of the thicker regions and the thinner ones and was guided by the presence of the topographic structure. In particular the submicron sized dot arrays between lines were fabricated with ease when the dewetting is confined into geometry with a few microns in size. As a simple application of our method, the controlled pattern on the transparent glass substrate was utilized for both circular and non-circular microlens arrays with the capability of modulating the focal length of a microlens by annealing time and temperature.

Acknowledgments. This research was supported by "SYSTEM2010" project funded by the Ministry of Commerce, Industry and Energy of the Korean Government. This work was also supported by the Second Stage of Brain Korea 21 Project in 2006, Seoul Research and Business Development Program (10816). and the Korea Science and Engineering Foundation (KOSEF) grant funded by the Korea government (MOST)(No. R11-2007-050-03001-0).

References

(1) S. J. Lee, Y. Son, C. H. Kim, and M. Choi, *Macromol. Res.*, **15**, 348 (2007).
(2) Y. J. Yu, S. H. Lee, D. H. Choi, J. I. Jin, and N. Tessler, *Macromol. Res.*, **15**, 142 (2007).
(3) C. H. Jang, *Macromol. Res.*, **15**, 263 (2007).
(4) N. Lu, X. Chen, D. Molenda, A. Naber, H. Fuchs, D. V. Talapin, H. Weller, J. Muller, J. M. Lupton, J. Feldmann, A. L. Rogach, and L. Chi, *Nano Lett.*, **4**, 885 (2004).
(5) M. Cavallini, J. Gomez-Segura, C. Albonetti, D. Ruiz-Molina, J. Veciana, and F. Biscarini, *J. Phys. Chem. B*, **110**, 11607 (2006).
(6) C. P. R. Dockendorf, T. Choi, and D. Poulikakos, *Appl. Phys.*

Lett., **88**, 131903 (2006).
(7) B. K. Yoon, J. Huh, H. C. Kim, J. M. Hong, and C. M. Park, *Macromolecules*, **39**, 901 (2006).
(8) P. F. Green, *J. Polym. Sci. Part B: Polym. Phys.*, **41**, 2219 (2003).
(9) X. Li, Y. Han, and L. An, *Polymer*, **44**, 5833 (2003).
(10) G. T. Carroll, M. E. Sojka, X. G. Lei, N. J. Turro, and J. T. Koberstein, *Langmuir*, **22**, 7748 (2006).
(11) M. L. Chabinyc, W. S. Wong, A. Salleo, K. E. Paul, and R. A. Street, *Appl. Phys. Lett.*, **81**, 4260 (2002).
(12) K. Y. Suh and R. Langer, *Appl. Phys. Lett.*, **83**, 1669 (2003).
(13) L. J. Heyderman, H. Schift, C. David, J. Gobrecht, and T. Schweizer, *Microelectronic Engineering*, **54**, 229 (2000).
(14) F. Brochard-Wyart, G. Debregeas, R. Fondecave, and P. Martin, *Macromolecules*, **30**, 1211 (1997).
(15) S. Qu, C. J. Clarke, Y. Liu, M. H. Rafailovich, J. Sokolov, K. C. Phelan, and G. Krausch, *Macromolecules*, **30**, 3640 (1997).
(16) P. Lambooy, K. C. Phelan, O. Haugg, and G. Krausch, *Phys. Rev. Lett.*, **76**, 1110 (1996).
(17) M. H. Wu, C. Park, and G. M. Whitesides, *Langmuir*, **18**, 9312 (2002).
(18) P. M. Moran, S. Dharmatilleke, A. H. Khaw, K. W. Tan, M. L. Chan, and I. Rodriguez, *Appl. Phys. Lett.*, **88**, 041120 (2006).
(19) S. Scheinert, G. Paasch, M. Schödner, H. Roth, S. Senssfuß, and T. Doll, *J. Appl. Phys.*, **92**, 330 (2002).